

Estimation of greenhouse gas emission due to open burning of rice straw using Sentinel data

Nguyen Cong Giang¹, Nguyen Quyet Chien^{2*}, Dang Vu Khac²

¹*Faculty of Civil Engineering, Hanoi Architecture University, Hanoi, Vietnam*

²*Faculty of Geography, Hanoi National University of Education, Hanoi, Vietnam*

Received 06 March 2024; Received in revised form 8 April 2024; Accepted 03 May 2024

ABSTRACT

In recent decades, Vietnam has gradually become a critical global rice producer. During that production process, residual straw becomes an environmental pollutant due to open burning, raising greenhouse gas emissions. This study combines the optical images of the Sentinel-2 satellite and the radar images of the Sentinel-1 satellite to estimate the dry biomass of rice and to determine gas emissions due to rice straw burning over the fields in Quoc Oai district, Hanoi city for urban environmental management purposes. Sentinel-2 images have been classified into the land covers, thereby identifying the areas of rice cultivation and the areas of burned straw. Meanwhile, the Sentinel-1 radar image has been used to calculate the dry biomass of rice due to its ability to penetrate clouds, an obstacle to optical images in tropical regions.

Furthermore, a field trip during harvesting season allows us to measure aboveground dry biomass. Then, the analysis shows a high correlation between the backscatter V.V. and V.H. of the radar image and the in-situ dry biomass ($R=0.923$ and $R^2=0.852$), with a relatively low average error (RMSE = 6.58 kg/100 m²). By linear regression method, the study found the total rice dry biomass of 28728.5 tons, which was obtained after the Summer rice crop 2020 for the whole Quoc Oai district, of which 2037.91 tons of rice straw have been burned, releasing a large amount of greenhouse gas emission with 2398.6 tons of CO₂, 189.5 tons of CO, 18.8673 tons of PM₁₀ dust, 17.2087 tons of PM_{2.5} dust and some other gases. The identical procedure has also been applied to the western region of Hanoi city center to estimate the amount of gas emissions. This study has proven the effectiveness of an approach and contributed to supporting urban managers in proposing appropriate policies to monitor and protect the environment.

Keywords: Straw burning, gas emission, regression, classification, Sentinel-1/2, dry biomass.

1. Introduction

Rice is one of the grains that plays a vital role in ensuring food security, and it is the main ration plant in many countries, including Vietnam. The International Food Policy Research Institute (IFPRI) analysis shows that the rice demand has increased by about 1.8%

per year (Ndikumana et al. 2018). The achievements in rice production have helped Vietnam ensure domestic consumption and put aside a considerable amount to export. The rice crop has also been cultivated in two major deltas (Red River Delta and Mekong River Delta), including Quoc Oai district, located about 20 km from the center of Hanoi city (Fig. 1). Quoc Oai has a large area of

*Corresponding author, Email: chiennq@hnue.edu.vn

agricultural land, of which 53.6% is for rice cultivation (Quoc Oai 2013; Vi, 2021). However, rice production activities also affect the environment when residual products, such as rice straw generated after harvesting, have not been adequately treated. They are abolished by burning in the fields (Minh 2021; Minh 2020).

Moreover, the rice straw is often not completely dry, so when burned, it forms smoke that covers large rural regions. Sometimes, smoke is carried away by the

wind, penetrating the residential areas of Hanoi's urban center. Burning rice straw causes many harms. Still, they mainly contribute to air pollution, creating greenhouse gases and bringing several potential health problems for the surrounding area's vulnerable population (Chang et al. 2012; Minh 2020). This issue has been considered in air quality monitoring programs of many countries, including Vietnam, but the habit of burning rice straw after harvesting has remained in Hanoi's rural districts.

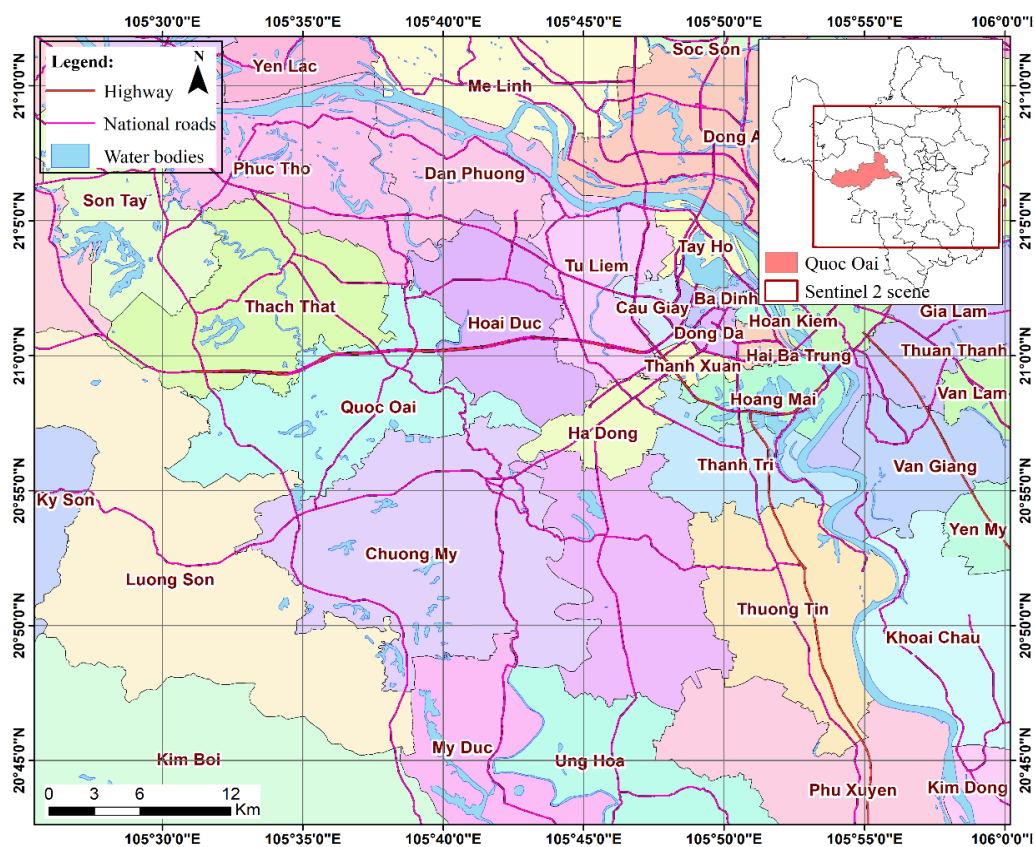


Figure 1. Administrative Boundary

Currently, the inventory of gas emissions from burning agricultural residues has faced many difficulties, especially in collecting data, due to several reasons such as the large surveying area, the limitation of budget, the lack of human resources, the lack of

observation equipment, etc. Therefore, an effective method is necessary to solve these issues at a reasonable cost and with high reliability for controlling and protecting air quality. In the major rice-growing regions of the world, several studies have been

conducted using satellite images to investigate the greenhouse gas emissions from burning agricultural residues (Chang et al. 2012; Kanabkaew and Nguyen 2011). In these studies, scientists have applied several approaches for estimating rice aboveground biomass, one of which commonly used the regression analysis by correlating rice dry biomass obtained from in-situ measurement with backscatter values obtained from radar images because this approach has reduced costs, time duration, and less impact on ground vegetation (Kumar et al. 2015; Ndikumana et al. 2018; Sodhi 2019).

In addition, Chih-Hua Chang has developed a method based on the classification of Formosat-2 satellite images acquired during the rice harvest season for mapping burned areas. This approach provides a practical and feasible solution to determine the areas of burned zones accurately (Chang et al. 2012). However, the gas emission inventory by this method has depended on the availability of rice production data, and the author did not consider the difference between rice variety and rice productivity across different localities. Harsimran Singh Sodhi worked on estimating rice aboveground biomass (AGB) with a combination of optical and radar data (Sodhi 2019). The results show that radar images were an adequate source for this purpose because they can capture longitudinal structural features and overcome weather constraints. However, radar images were not a reasonable choice for distinguishing vegetation categories like optical images. Therefore, it is possible to combine radar and optical images to improve the accuracy of rice biomass estimation (Sodhi 2019).

In Vietnam, many researchers have used remote sensing and GIS techniques for investigating forest fires over the last decades (Luu et al. 2014; Pham et al. 2024; Tran et al. 2023), and they have also exploited satellite images to estimate forest biomass (Nguyen et

al. 2014). However, the estimation of dry rice biomass and the amount of gas emission is still a novel issue, as shown by several research studies by Pham Thi Mai Thao (2019) and Le Hoang Anh (2020), among others. In Pham Thi Mai Thao's study, data relating to the areas of rice cultivation and its productivity were gathered from the Statistical Yearbooks and used for estimating gas emissions. The amount of straw was collected according to the samples to calculate the average weight of straw (kg/m^2), and the percentage of straw utilization was based on a survey conducted by local people (Pham 2019). This method also has limitations because it does not show the spatial variation of results to find solutions for each locality. The selection of samples and rice productivity for estimating the amount of rice straw after harvest is also tricky because it depends on rice variety, level of fertilization practice, soil categories, climate, irrigation conditions, and specific crops in each region.

Otherwise, the percentage of households who burn rice straw depends on the number of surveyed households. In Le Hoang Anh's study, the authors used the Sentinel-1 images to estimate the areas of rice cultivation and its productivity for each locality. The authors applied the formula to calculate total gas emissions based on the obtained data. The results show that backscatter values from radar images strongly correlate with rice productivity and aboveground biomass (Lê et al. 2020). However, the authors based their calculation on the percentage of residual products and combustion efficiency from published studies in some Asian countries such as Thailand and China to calculate the amount of burned biomass. However, this approach has several limitations due to the different agricultural practices between countries.

Since 2015, the European Space Agency (ESA) has launched Sentinel-1 and Sentinel-2 satellites into orbit to capture Earth's surface images. The images of these satellites have been widely used in natural resource

management and environmental monitoring (Nguyễn et al., 2018). Sentinel-2 satellite images can be exploited to determine the rice occupation in fields. Meanwhile, Sentinel-1 satellite images have also become a common choice in estimating rice aboveground biomass because they can overcome weather limitations that optical satellite images have often encountered (Lê et al. 2020; Ndikumana et al. 2018; Nguyễn et al. 2018). The simultaneous use of the optical image of the Sentinel-2 satellite and radar image of the Sentinel-1 satellite, together with in-situ measurement data, allows this study to estimate dry rice biomass for calculating the amount of greenhouse gas emissions, which were arising from the open burning of rice straw in Quoc Oai district, Hanoi city. The results contribute to proposing appropriate policies for converting biomass into energy or other products or effectively controlling gas emissions from the rice production process for sustainable development.

2. Method and used data

2.1. Used data and processing steps

2.1.1. Satellite images

Two types of satellite data are used: optical and radar images.

Radar images: the Sentinel-1 satellite provides radar images with a repeat cycle of 12 days and a spatial resolution of 10 m. Microwaves are highly sensitive to some parameters, such as the ground surface's roughness, the vegetation's structure and orientation, and the moisture content (Lê 2005). In addition, the sensitivity of Sentinel-1 polarizations was investigated for bare soil or vegetation-covered surfaces. For monitoring crops in general and estimating biomass in particular, radar images are compelling in tropical regions with heavy rainfall (Nguyễn 2021). This study used Sentinel 1 image captured on 21 September 2020 to estimate the dry biomass of rice over

the Quoc Oai district - a study area located in the west of Hanoi. Level 1 with orbital data was applied to the selected image, of which phase values have been replaced by the intensity and amplitude components. Still, this radar image has not been georeferenced, and the speckle noise has not been filtered yet.

Optical images: the Sentinel-2 offers optical images with which the land cover categories are determined through the reflectance values. These images have been pre-processed at level 2A by NASA with a transformation from D.N. values to reflectance ones, and they have been georeferenced in the UTM-WGS84 coordinate system. The Sentinel-2's bands have different spatial resolutions, but raster-based analysis demands all bands at the identical dimension. That is why we have enhanced all existing spectral bands with 20 m and 60 m dimensions to the higher resolution of 10 m, preserving their reflectance with convolution neural network methods (Galar et al. 2020). In this study, a cloud-free optical scene during the Summer period is limited because of cloud coverage over this region; a multispectral image taken on 26/08/2020 was used to identify the spatial distribution of rice cultivation for the Summer rice crop in Quoc Oai district on the one hand. In 2020, the Summer rice crop started in July and finished in October, when most rice fields were harvested. That is why the image taken on 9/11/2020 was used to determine the spatial distribution of burned rice fields.

Google Earth images: Google Earth integrates several types of spatial data, including satellite images, which can be displayed over time using historical imagery, and provided images can reach an ultra-high spatial resolution of <1.0 m (Malarvizhi et al., 2016). The image taken in June 2020 was chosen to select validation samples, and the interpreter can easily recognize land cover categories based on actual knowledge acquired through field surveys.

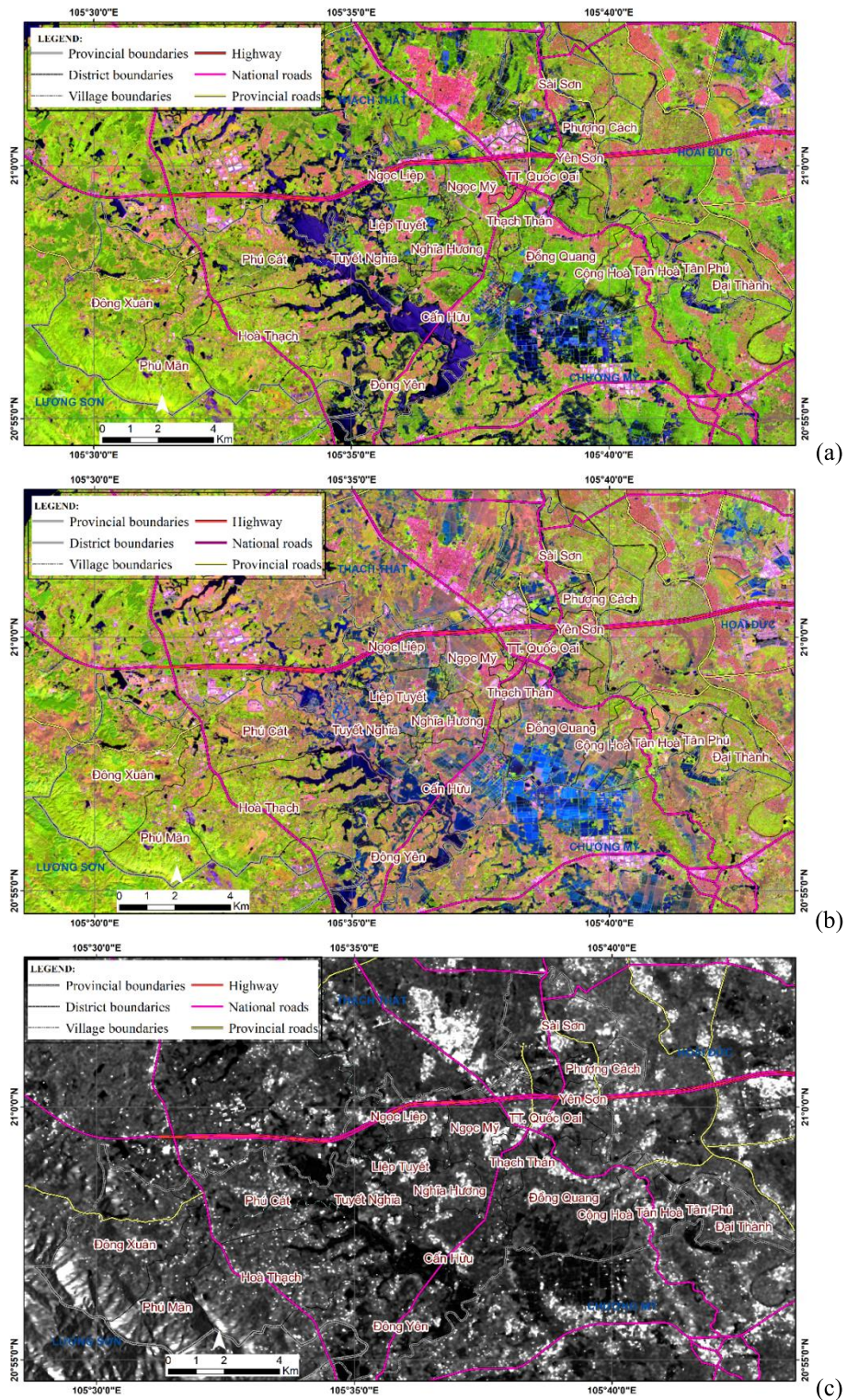


Figure 2. (a) Color composite (b11-b8-b2) of Sentinel-2 on 26 August 2020; (b) Sentinel-2 on 09 November 2020; (c) Sentinel-1 on 21 September 2020

2.1.2. In-situ measurement

The dry biomass data (rice straw) has been collected at 30 standard plots (OTC) in Quoc Oai district (each OTC corresponds to one pixel 10×10 m with an area of 100 m²). The in-situ measurement was carried out during

the harvesting the Summer rice crop in October 2020 (Fig. 3). Each OTC's rice plant has been cut from bottom to top, and rice grains have been removed. The rice straw was conventionally dried under sunlight and then weighed to identify its weight (kg).



Figure 3. Harvesting rice in the standard plot (OTC) at Can Huu commune

2.1.3. Processing steps

The schematic diagram shows how to handle data in this research: image cropping, spatial resolution enhancement, color combination, training sample selection, the

Support Vector Machine -SVMs image classification, noise filtering, vector transformation, accuracy assessment, analysis, and result validation. Some main steps are presented in the Fig. 4.

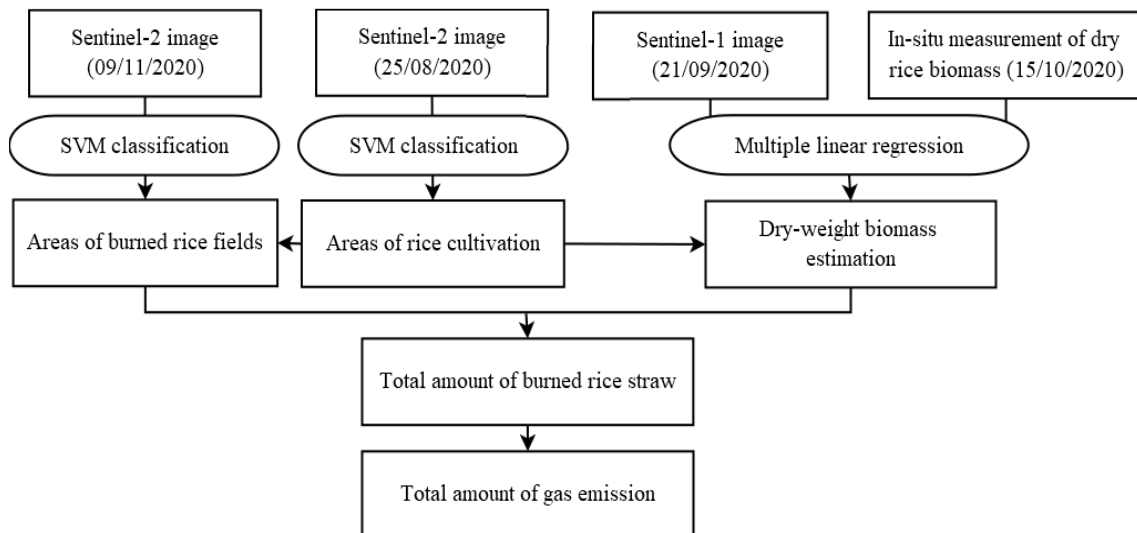


Figure 4. Main processing steps applied in this study

2.2. Identifying the amount of rice dry biomass

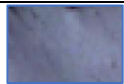
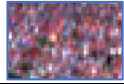
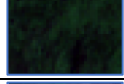



2.2.1. Areas of rice cultivation

* Selection of training samples

Before supervised classification, the training samples were identified by selecting from the natural color composite of multispectral bands with visual interpretation criteria. A set of samples (ROIs) for each land cover category was selected with an average

of 300 pixels corresponding to each sample. Then, the separability between different land cover categories was calculated, providing a good result in values ranging from 1.9 to 2.0. Table 1 shows the samples of significant land cover categories in the study area, where the color and texture of each sample represent the different categories of land cover, including water bodies, residences, forests, rice fields, grassland, and bare soil.

Table 1. Training samples are selected from natural color composite (B4, B3, B2)

| No | Land cover | Description | Sentinel-2 |
|----|------------|--|---|
| 1 | Waterbody | Light blue or purple color. The texture is relatively smooth. They have clear shapes. |  |
| 2 | Residence | Deep pink color and patchy texture. They distribute along traffic routes and often intersperse with vegetation. |  |
| 3 | Forest | Dark green color very rough texture. They include natural forests, plantations, and orchards. |  |
| 4 | Grassland | Light green color, smooth texture. They often concentrate around waterside areas, where rice fields transfer to forest land. |  |
| 5 | Rice field | Very dark green or black color. The texture is relatively homogeneous. The boundaries are pretty clear. |  |
| 6 | Bare soil | Brown, light yellow color. Distributed mainly along roadsides, where there are construction works, mining areas. |  |

* Image classifier using SVMs algorithm

To determine the area of Summer rice cultivation in Quoc Oai district, the SVMs classifier algorithm has been applied to Sentinel-2 images. Currently, the SVM algorithm is quite commonly implemented in satellite image classification to simultaneously map land use/land cover categories in urban and suburban areas (Nemmour and Chibani 2006; Xiong et al. 2010). Although it has been developed for about three decades, the results of recent studies have demonstrated the superiority of SVMs over other standard classifier algorithms due to their ability to generalize across various objects of interest despite a limited training sample set (Colas

and Brazdil 2006; Medina and Atehortúa 2019; Mountrakis et al. 2011). Moreover, Paneque-Gaslvez et al. (2013) noted that the SVMs algorithm accurately maps land cover categories in a large, heterogeneous tropical region (Paneque-Gálvez et al. 2013).

2.2.2. Dry rice biomass

The purpose of regression analysis is to find out the relationship between one variable (often called the dependent variable) and one or several other variables (often called the independent variable) for estimating or predicting the expected values of the dependent variable when the value of independent variables is known in advance

(Phạm 2015). This study used the method of multivariable linear regression analysis for identifying the correlation between dry rice biomass with the backscatter coefficients at V.V. and V.H. polarization of Sentinel-1 image, thereby giving a model that allows to estimate the amount of dry rice biomass as the following equation:

$$B = X_0 + X_1 \times R_{VV} + X_2 \times R_{VH} \quad (1)$$

Where B is dry rice biomass, R_{VV} and R_{VH} are backscatter coefficients in decibels. X_0 , X_1 , and X_2 are coefficients determined by correlation analysis based on in-situ measurement data and satellite image data at the same position. R_{VV} and R_{VH} are independent variables, while dry rice biomass measured in the rice field is considered dependent. The weight of dry rice biomass in 25 OTCs among 30 OTCs was used for linear regression analysis, and the remaining data in 5 OTCs were considered to validate the model. The model was chosen based on the

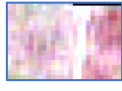





correlation coefficient (R) and the square root of the mean error (RMSE) between the measured and calculated data.

2.3. Estimating gas emissions by burning of straw

2.3.1. Areas of burned rice straw

Identifying the area of burned rice fields after harvest has several limitations, and its accuracy is not sufficiently adequate. Traditional survey methods provide deficient spatial coverage. In addition, the survey results may also comprise some biases due to the subjective opinions of surveyors. Classifying multispectral images provides an alternative approach, which allows us to directly detect the burned zones through the specific color of burned straw on satellite images (Table 2). This method has a considerable advantage because it can be easily applied to almost all optical satellite images.

Table 2. The characteristics for visual interpretation of burned rice fields

| No | Land covers | Description | Sentinel-2 | Survey photos |
|----|-------------|---|---|---|
| 1 | A | Harvested but no other activities, no burning of straw, and no grass growing back |  |  |
| 2 | B | Harvested and covered by weeds |  |  |
| 3 | C | Harvested and burned rice straw |  |  |

Furthermore, the accuracy of image classification at a regional scale can be enhanced by exploiting high spatial resolution images and available GIS data. By applying the super-resolution model, multispectral bands of Sentinel-2 images have been improved to reach a finer spatial resolution (10 m × 10 m), allowing the identification of the burned areas accurately. However, due to the complexity of

human activities, a set of different land cover categories can include different land use (e.g., residential land or agricultural land) or designated land use stages (e.g., paddy fields or harvested rice fields) or special activities on the ground (e.g., burned rice fields or unburned rice fields). To obtain vital information regarding RSOB (rice straw open burning) and improve the overall accuracy of classification,

the number of categories has been limited using classified rice cultivation boundaries obtained in the previous section 2.2.1. After limiting the classification target, the SMVs classifier was again applied to the second Sentinel-2 image using training samples issued from visual interpretation for identifying burned rice fields.

2.3.2. Gas emission from Summer rice crop in 2020

Estimating gas emissions from the burning of rice straw is based on the quantity of rice straw burned and the emission coefficients (E.F.). In this study, the amount of gas emissions was estimated using the following formula (3) (Kanabkaew and Nguyen 2011):

$$Em_{ij} = \sum_j^n M_j \times EF_{ij} \quad (2)$$

Where: i is pollutant i ; j is plant j ;

Em_{ij} is the emission of pollutant i from plant j ;

M_j is the burned biomass from plant j (kg/year);

EF_{ij} is the emission coefficient of pollutant i from plant j (g/kg).

Accordingly, the emission coefficients (g/kg) of some emitted gases by the burning of rice straw are shown in Table 3 (Lê et al., 2020).

Table 3. Emission coefficient of pollutants (g/kg)

| No | Pollutants | Emission coefficients (EF _{ij}) | No | Pollutants | Emission coefficients (EF _{ij}) |
|----|-------------------|---|----|-----------------|---|
| 1 | PM ₁₀ | 9.1 | 4 | CO | 93 |
| 2 | PM _{2.5} | 8.3 | 5 | NH ₃ | 4.1 |
| 3 | CO ₂ | 1177 | 6 | CH ₄ | 9.59 |

3. Results







3.1. Areas of rice cultivation and areas of burned rice straw

* Validation

Image classification results can be affected by various factors, such as the classification approach, the algorithm used, and the configuration of the satellite image. In this study, the accuracy of the SVMs classifier using Sentinel-2 images was independently estimated based on the validated samples selected by visual interpretation of Google Earth images captured during the same season (June 2020) (Labib and Harris, 2018). A field survey was also conducted in October 2020 to compare the obtained classes with objects on the ground.

Table 4 presents validated samples collected through visual interpretation using several criteria: position, structure and shape, tone/color, and association (Estes, Hajic, & Tinney, 1983). Land cover categories can be identified due to the high spatial resolution of Google Earth images. The validation dataset includes 12 samples with an average of 300 pixels/sample for each land cover category.

Table 4. Validation samples of land cover were selected from Google Earth image

| No | Land cover | G.E. | No | Land cover | G.E. |
|----|--------------|---|----|------------|---|
| 1 | Water bodies |  | 4 | Grassland |  |
| 2 | Residence |  | 5 | Rice field |  |
| 3 | Forest |  | 6 | Bare soil |  |

The accuracy of classification is considered through the error matrix and

Kappa index (Cohen 1960). Sentinel-2 image captured on 26 August 2020 has been used for

determining the spatial distribution of rice cultivation land, and it has provided an overall accuracy of 86.31% (3338374/3867696) with a Kappa index of 0.81. The Sentinel-2 image captured on 9 November 2020 has been exploited for identifying the spatial distribution of burned rice fields, and it has offered an overall accuracy of 89.19% (3797907/3867696) with a Kappa index of 0.85. From the mentioned results, it is shown that the overall accuracy and the Kappa index are adequate, respectively ($> 80\%$ and $k > 0.8$)

for reliable results (Wilhelm 2008).

** Comparison with high spatial resolution images*

To validate the obtained SVMs classification, the contour of the rice cultivation land extracted from the Sentinel-2A image (26 August 2020) was overlaid on the Google Earth image (June 2020). The two random frames in Fig. 5 show the geometric and thematic match between the two datasets in the validation context.

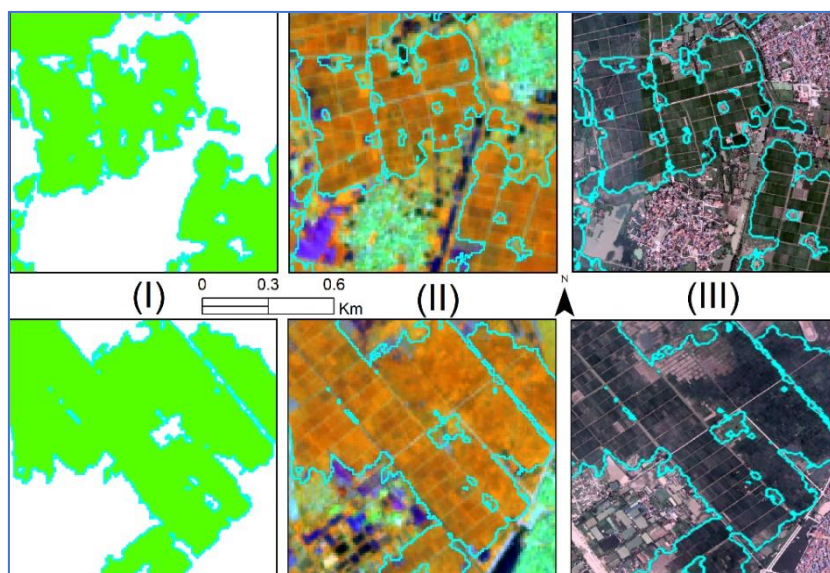


Figure 5. Comparison of rice cultivation extracted from Sentinel-2A and G.E. image: (I) Rice extracted from Sentinel-2A. (II) Color composite (B8, B11, B4) of Sentinel-2A image. (III) Extracted rice overlays on G.E. image. For the location of frames, refer to Fig. 6

** Spatial distribution*

From the classification results using the SVMs classifier, we can map the area of rice cultivation land (Fig. 6a) and the area of burned rice fields in Quoc Oai during the harvesting of Summer rice crops in 2020 (Fig. 6b).

Obtained statistical data on the area of burned rice fields by commune are presented in Fig. 7. The analysis shows that Dong Quang commune has the most significant

areas of burning rice straw (34.41 ha), followed by Ngoc Liep commune (28.41 ha) and Can Huu commune (23.47 ha). These are also communes with a large rice cultivation area in the Quoc Oai district. Some communes have relatively small areas of burning rice straw, such as Tan Phu (0.08 ha), Hoa Thach (0.4 ha), Phu Man (0.6 ha), and Yen Son (0.66 ha). Due to the tiny rice cultivation land, only Dai Thanh commune has almost no burned rice area.

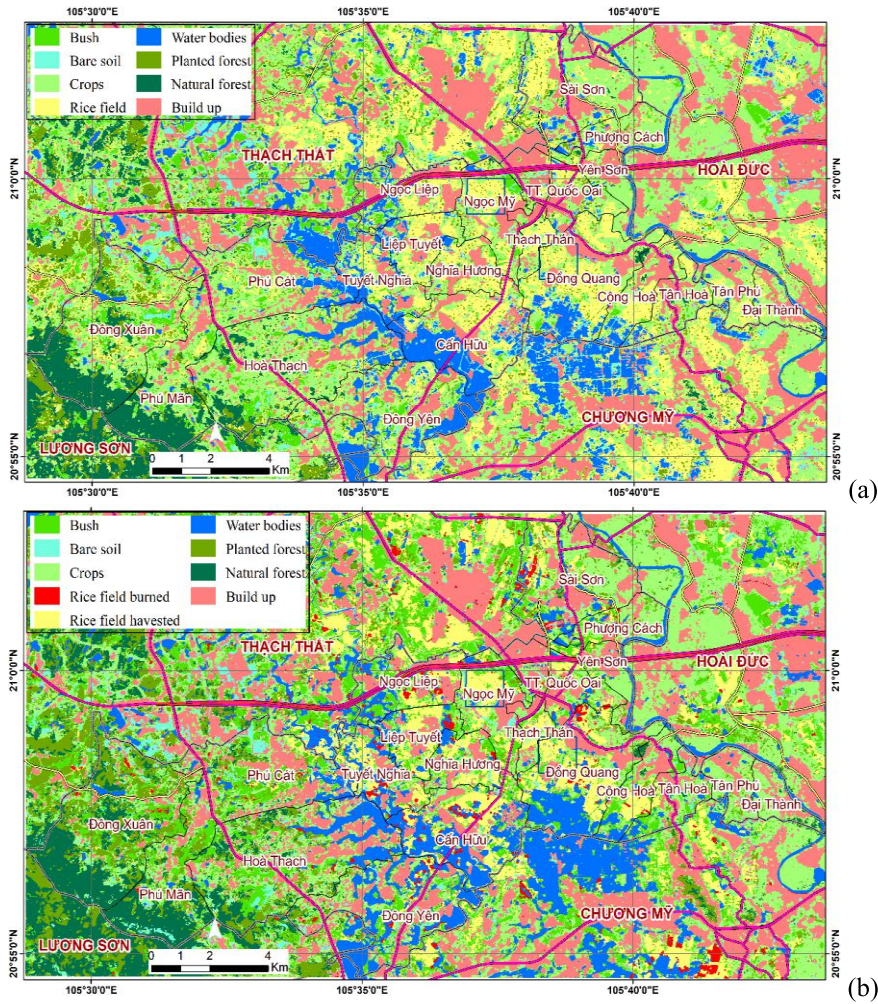


Figure 6. Summer rice crop of Quoc Oai district in 2020:
 (a) Distribution of rice cultivation land issued from Sentinel 2 (26 August 2020);
 (b) Distribution of burned rice fields issued from Sentinel 2 (09 November 2020)

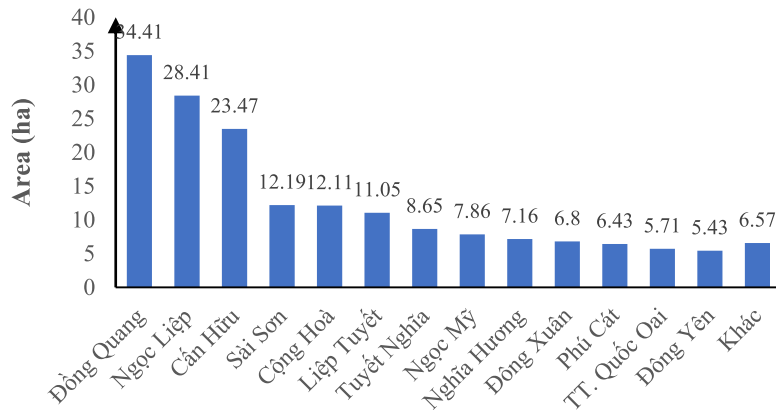


Figure 7. Allocation of area from burning straw by the communes for Summer rice crop in 2020

3.2. Dry rice biomass

The analysis of the regression model between dry rice biomass with backscatter on radar image (Phạm 2015), the amount of dry rice biomass, which dual polarization V.V. and V.H. calculated, shows a high correlation coefficient ($R=0.923$ and $R^2=0.852$) and relatively low mean error (RMSE= $6.58 \text{ kg}/100 \text{ m}^2$), it can be noted that dry rice biomass and backscatter response V.V. and V.H. of Sentinel-1 image are highly

correlated. The regression equation to calculate the weight of dry rice biomass has the following form:

$$B = 24.60 + 361.75 \times R_{VV} + 1210.54 \times R_{VH} \quad (3)$$

We applied correlation model (3) to calculate dry rice biomass for each pixel of the Sentinel-1 image (100 m^2). The area of rice land cultivation was then used to separate the rice biomass value from the ones of other land cover categories. The obtained results are shown in Fig. 8.

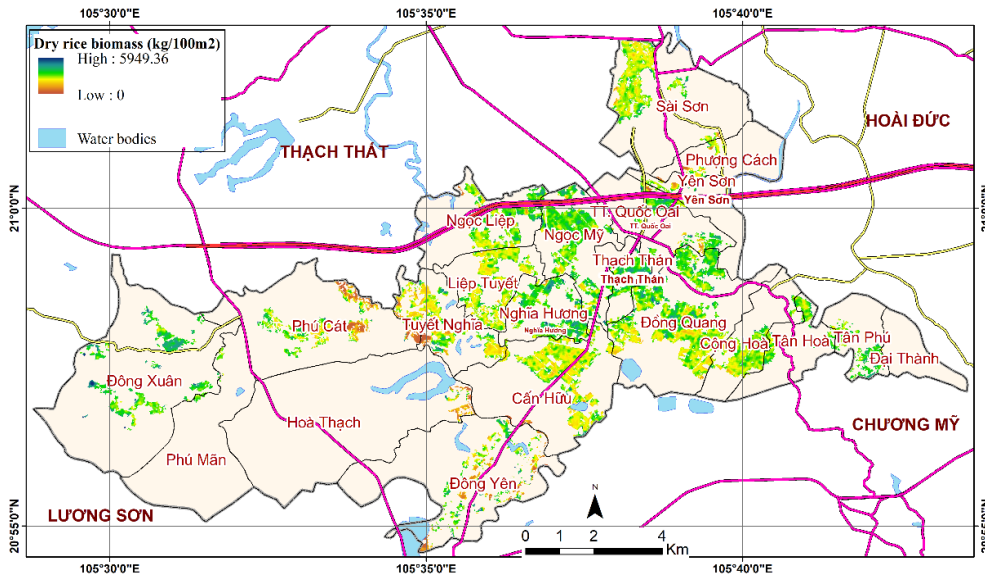


Figure 8. Dry rice biomass of each pixel for the Summer rice crop of Quoc Oai district ($\text{kg}/100 \text{ m}^2$)

The obtained map shows that the dry rice biomass of Quoc Oai district mainly ranges from 50 to $200 \text{ kg}/100 \text{ m}^2$ because the amount of dry rice biomass depends on the rice variety, fertilization level, soil type, climate,

irrigation conditions, and season (Pham 2019). After obtaining the rice biomass per pixel, data from the remaining 5 OTCs was analyzed to validate the model; the results are shown in Table 5.

Table 5. Comparison of rice biomass issued from different data sources

| No | Dry rice biomass issued from in-situ measurement ($\text{kg}/100 \text{ m}^2$) | Dry rice biomass issued from radar image ($\text{kg}/100 \text{ m}^2$) | Error ($\text{kg}/100 \text{ m}^2$) |
|----|--|--|---------------------------------------|
| 1 | 107.0 | 104.4 | -2.6 |
| 2 | 113.0 | 99.8 | -13.2 |
| 3 | 116.0 | 107.0 | -9.0 |
| 4 | 89.0 | 92.8 | 3.8 |
| 5 | 83.0 | 92.9 | 9.9 |

The above comparison shows a high correlation between dry rice biomass collected

from the field and dry rice biomass calculated from satellite images. The mean error of

2.18% is acceptable with a root mean square error (RMSE) of 11.1 kg/100 m².

The total rice biomass per pixel was calculated, and thereby, the total dry rice biomass of Quoc Oai district for the Summer rice crop 2020 was 28728.53 tons, with an average of 112.63 kg/100m². This amount is equivalent to 11.26 tons/ha, of which 2037.91 tons of rice straw were directly burned on the field.

3.3. Amount of gas emission from burning activity on rice fields

After determining the area of burned rice fields and the weight of dry rice biomass per pixel, the amount of burned rice biomass of 2037.91 tons can be identified. Since then, the amount of gas emission from the burning of rice straw has been determined through the formula (2). The total emissions are shown in Table 6 and demonstrated for each commune (Table 7).

Table 6. Amount of gas emissions after harvesting Summer rice crop in 2020

| No | Pollutants | Emitted volume (tons) | No | Pollutants | Emitted volume (tons) |
|----|-------------------|-----------------------|----|-----------------|-----------------------|
| 1 | PM ₁₀ | 18.8673 | 4 | CO | 189.5182 |
| 2 | PM _{2.5} | 17.2087 | 5 | NH ₃ | 8.5007 |
| 3 | CO ₂ | 2398.6086 | 6 | CH ₄ | 19.8833 |

Table 7. Allocation of gas emissions from burning straw by the communes of Quoc Oai district for Summer rice crop in 2020 (tons)

| Commune name | PM ₁₀ | PM _{2.5} | CO ₂ | CO | NH ₃ | CH ₄ |
|--------------|------------------|-------------------|-----------------|----------|-----------------|-----------------|
| Quốc Oai | 493.60 | 450.21 | 63842.08 | 5044.45 | 222.39 | 520.18 |
| Phú Mãn | 68.04 | 62.06 | 8799.21 | 695.26 | 30.65 | 71.70 |
| Phú Cát | 665.23 | 606.75 | 86038.47 | 6798.52 | 299.72 | 701.05 |
| Hoà Thạch | 32.87 | 29.98 | 4251.81 | 335.95 | 14.81 | 34.64 |
| Tuyết Nghĩa | 908.20 | 828.36 | 117466.76 | 9281.57 | 409.19 | 957.10 |
| Đông Yên | 568.58 | 518.60 | 73541.14 | 5810.81 | 256.18 | 599.20 |
| Liệp Tuyết | 1127.34 | 1028.24 | 145812.53 | 11521.30 | 507.93 | 1188.06 |
| Ngọc Liệp | 3265.29 | 2978.23 | 422334.96 | 33369.11 | 1471.18 | 3441.11 |
| Ngọc Mỹ | 680.14 | 620.35 | 87969.97 | 6950.89 | 306.44 | 716.76 |
| Cần Hữu | 2388.07 | 2178.13 | 308874.38 | 24405.54 | 1075.94 | 2516.66 |
| Nghĩa Hương | 903.06 | 823.67 | 116801.94 | 9229.04 | 406.87 | 951.68 |
| Thạch Thất | 126.51 | 115.38 | 16362.35 | 1292.79 | 57.00 | 133.32 |
| Đông Quang | 3886.23 | 3544.59 | 502647.86 | 39716.18 | 1750.94 | 4095.49 |
| Sài Sơn | 1264.13 | 1152.99 | 163502.88 | 12919.09 | 569.55 | 1332.19 |
| Yên Sơn | 55.00 | 50.16 | 7113.41 | 562.06 | 24.78 | 57.96 |
| Phượng Cách | 134.55 | 122.72 | 17401.76 | 1375.09 | 60.62 | 141.80 |
| Tân Phú | 8.87 | 8.09 | 1147.88 | 90.70 | 4.00 | 9.35 |
| Đại Thành | 0.00 | 0.00 | 0.00 | 0.00 | 0.00 | 0.00 |
| Tân Hoà | 78.95 | 72.01 | 10210.91 | 806.81 | 35.57 | 83.20 |
| Cộng Hoà | 1315.28 | 1199.65 | 170118.79 | 13441.84 | 592.60 | 1386.10 |
| Đông Xuân | 897.39 | 818.50 | 116069.49 | 9171.17 | 404.32 | 945.71 |

Table 6 shows the highest amount of CO₂ emitted from burning rice straw in Quoc Oai district (2398.6 tons/crop) because CO₂ is the main product of the combustion process. CO is a second product with 189.5 tons/crop because the rice straw is not completely dry or

burned in high-humidity weather conditions. Fine dust PM10 and PM2.5 also have high concentrations due to incomplete combustion. Dong Quang, Ngoc Liep, and Can Huu communes are the main rice-producing communes of the district, so they have a large

area of burned rice straw with a considerable amount of gas emissions. These communes have many favorable conditions in terms of land, topography, and water resources. They are all located along significant traffic roads with rapid urbanization. Otherwise, the demand for straw for cooking is not so high. Therefore, the burning of rice straw takes place in fields to a large extent.

Meanwhile, some communes in the west, such as Hoa Thach, Dong Xuan, Phu Cat, and Phu Man, occupy a large area. Still, the amount of gas emissions from burning rice straw is not crucial because these communes are located in landforms with high elevations, mainly hilly areas with degraded soil, unfavorable for rice cultivation. Farmers mainly grow corn, tea, or other fruit trees in these communes.

3.4. Discussions

Quoc Oai is a rural district of Hanoi city, located in the transitional region between mountains and plain, for nearly 90% of the population living in rural areas. The results show that after the Summer rice crop of 2020, Quoc Oai district yielded 26570.63 tons of rice straw, of which 2037.91 tons have been burned, accounting for more than 7%. It is still a significant number in the overall goal of Hanoi city of no longer burning rice straw by 2020 (Quân 2019). This activity has emitted an amount of gas emissions, including 2398.6 tons of CO₂, 189.5 tons of CO, 18.8673 tons of PM₁₀ dust, 17.2087 tons of PM_{2.5} dust, and several other gases.

Otherwise, the area of rice cultivation land in the eastern region of Hanoi city has been reduced due to urbanization. In contrast, rice fields have considerably remained in the western region along the floodplain of Day River, including the Quoc Oai district. At

these places, rice straw burning activity has gradually occurred and caused toxic agents that have affected local air quality, the surrounding area, and the inner city. Therefore, the identical treatment procedure mentioned in the above section has been applied to identify the amount of dry rice biomass during the harvest season of summer rice crops in this broad region to reduce gas emissions. Figure 9 shows the location of rice cultivation land for Summer rice crops in 2020 (73880.1 ha). These rice fields yielded a total of 193777.37 tons of dry rice biomass. The area of burned rice fields (4018.4 ha) is aggregated in large patches in rural districts such as Quoc Oai, My Duc, Chuong My, and Ung Hoa. Burning rice straws in Vietnam is also happening in other localities, causing severe air pollution, and the situation is forecasted to worsen over the coming years if the regulations are not effectively managed by modern tools such as remote sensing.

However, rice straw is a valuable resource, and its use as a raw material is recommended instead of burning. It could be converted for many purposes, such as animal feed preparation (Mai 2011), mushroom cultivation (Nguyễn 2018), organic fertilizer, hydrogen production (Morya et al. 2023), construction materials - ultra-lightweight concrete (Ta et al. 2010), biomass briquette (Hossen et al. 2019), charcoal briquette (Narzary et al. 2023), bioethanol production (Takano and Hoshino 2018), or straw pulp and paper-making (Kaur et al. 2017). Therefore, monitoring greenhouse gas emissions due to burning is estimating the weight of dry rice biomass and the amount of gas emission after harvest to help authorities propose adequate policies that allow the wastage of biological resources to be avoided and minimize environmental pollution.

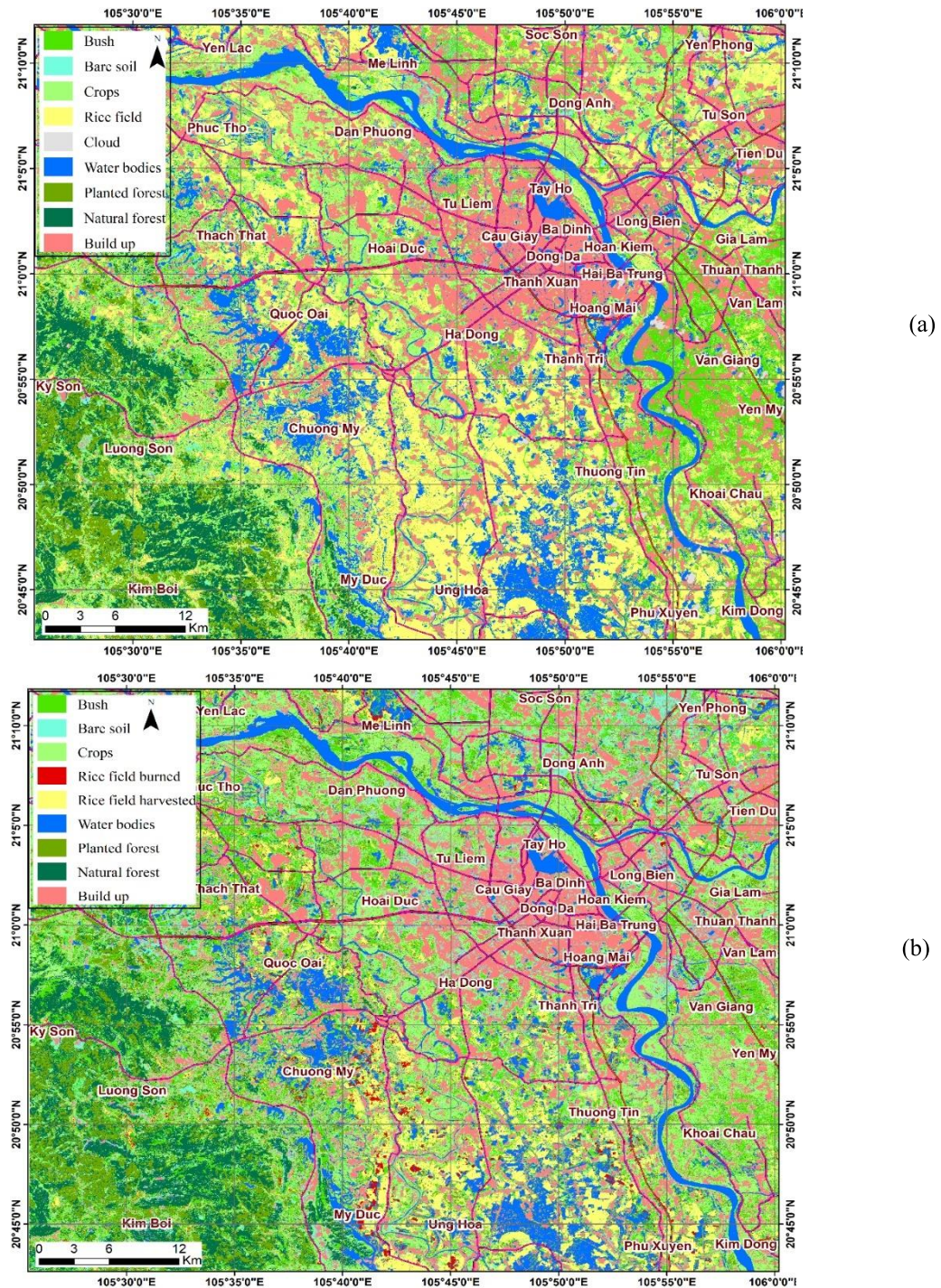
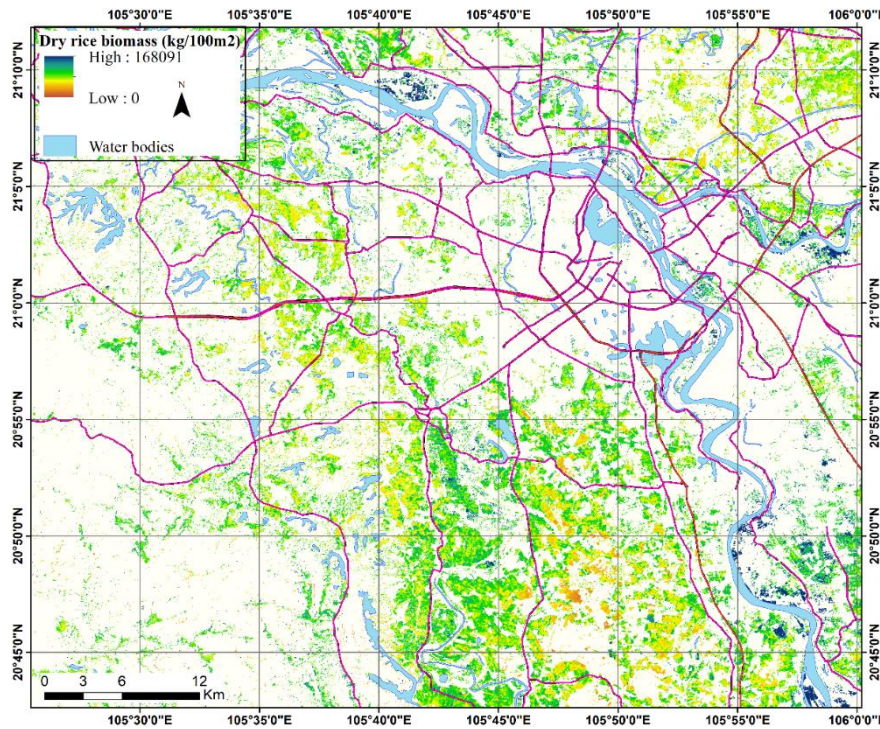


Figure 9. Summer rice crop of the western region in 2020:

- (a) Distribution of rice cultivation land issued from Sentinel 2 (26 August 2020);
- (b) Distribution of burned rice fields issued from Sentinel 2 (09 November 2020);
- (c) Dry rice biomass of each pixel ($\text{kg}/100\text{m}^2$) from Sentinel 1 (21 September 2020)



(c)

Figure 9. Cont.

4. Conclusions

With coefficient $R=0.923$ corresponding to $R^2=0.852$ and relatively low root mean square error ($RMSE=6.58 \text{ kg}/100\text{m}^2$), the results demonstrate that the weight of dry rice biomass and the values of V.V. and V.H. backscattering in Sentinel-1 image is strongly correlated. The regression analysis associated with the supervised classification methods can be applied to Sentinel 1/2 images to provide a reliable result, primarily when the survey must be carried out on a broad territory. Optical and radar images separately have advantages and disadvantages in monitoring rice crops. However, this study has realized their combination to overcome limitations and prove their benefits. This study shows that satellite data from the Sentinel hub (free of charge and free of use) is sufficient to accurately calculate the amount of gas emitted from burning straws. For this stage, the open burning of rice straw has been investigated at the district level. However, the study's

findings indicate the ability to adequately use identical techniques and methodologies when expanding to analyze data for a broader territory such as the western region of Hanoi city. Due to its adequate accuracy, the obtained information is meaningful for urban environment management, especially in reducing straw-burning emissions.

Acknowledgments

The authors acknowledge Hanoi Architecture University and Hanoi National University of Education for supporting this research. We acknowledge the European Space Agency for providing Sentinel images through the Copernicus data hub.

References

Center of Cultural Information and Sport of Quoc Oai district, 2013. General introduction of Quoc Oai district, Quoc Oai People Committee, Hanoi, accessed on 20 February 2023, at website <https://quocoai.hanoi.gov.vn/>.

- Chang C.-H., Liu C.-C., Tseng P.-Y., 2012. Emissions Inventory for Rice Straw Open Burning in Taiwan Based on Burned Area Classification and Mapping Using Formosat-2 Satellite Imagery. *Aerosol and Air Quality Research*, 13(2), 474–487.
- Cohen J.A., 1960. Coefficient of Agreement for Nominal Scales. *Educational and Psychological Measurement*, 20(1), 37–46.
- Colas F., Brazdil P., 2006. Comparison of SVM and Some Older Classification Algorithms in Text Classification Tasks. In M. Bramer (Ed.), *Artificial Intelligence in Theory and Practice*. Boston, MA: Springer US, 169–178.
- Estes J.E., Hajic E.J., Tinney L.R., 1983. Fundamentals of image analysis: Analysis of visible and thermal infrared data. In R. N. Colwell (Ed.), *Manual of remote sensing*. United States: American Society of Photogrammetry, 987–1124.
- Galar M., Sesma R., Ayala C., Albizua L., Aranda C., 2020. Super-Resolution of Sentinel-2 Images Using Convolutional Neural Networks and Real Ground Truth Data. *Remote Sensing*, 12(18), 2941.
- Hanoi is full of pollution due to burning rice straw. Tien Phong. Retrieved from <https://tienphong.vn/ha-noi-mit-mu-o-nhiem-do-dot-rom-ra-post1343910.tpo>, accessed on 15 June 2023.
- Hossen M.A., Bhuiyan M., Huda M.D., Ahiduzzaman M., Baki Z., Paul H., 2019. Prospect of rice straw biomass briquette production: an alternative source of energy. *Journal of Agricultural Engineering*, 42/AE(3), 79–86.
- Kanabkaew T., Nguyen T.K.O., 2011. Development of spatial and temporal emission inventory for crop residue field burning. *Environmental Modeling & Assessment*, 16453–464.
- Kaur D., Bhardwaj N.K., Lohchab R.K., 2017. Prospects of rice straw as a raw material for paper making. *Waste Management*, 60127–139.
- Kumar L., Sinha P., Alqurashi A.F., Taylor S., 2015. Review of the use of remote sensing for biomass estimation to support renewable energy generation. *Journal of Applied Remote Sensing*, 9(1), 1-28.
- Labib S.M., Harris A., 2018. The potentials of Sentinel-2 and Landsat-8 data in green infrastructure extraction, using object based image analysis (OBIA) method. *European Journal of Remote Sensing*, 51(1), 231–240.
- Le H.A., Nguyen V.T., Đỗ M.P., Hồ Q.B., Nguyễn Q.H., Đinh M.C., 2020. Inventory of gas generated by burning rice straw on the field at Hanoi city using Sentinel-1 satellite. *VNU Journal of Science: Earth and Environmental Sciences*, 37(1), 81–92.
- Le V.T., 2005. *Remote Sensing*. Ho Chi Minh city National University Publishing House, 419.
- Luu T.A., Tran A.T., Hoang T.H.N., Le B.B., 2014. Application of remote sensing imagery and GIS in establishment of forest fire hazard map in Daklak province. *Vietnam J. Earth Sci.*, 36(3), 252–261. <https://doi.org/10.15625/0866-7187/36/3/5908>.
- Mai T.T., 2011. Research on the use and management of rice straw towards sustainable agricultural development in Soc Son District, Hanoi. In, *University of Natural Sciences*. Hanoi: Hanoi National university, p.97.
- Malarvizhi K., Kumar S.V., Porchelvan P., 2016. Use of High Resolution Google Earth Satellite Imagery in Landuse Map Preparation for Urban Related Applications. *Procedia Technology*, 241835–1842.
- Medina J., Atehortúa B., 2019. Comparison of maximum likelihood, support vector machines, and random forest techniques in satellite images classification. *Tecnura*, 23(59), 13–26.
- Minh N., 2020. Warning about environmental pollution from burning straw. *Vietnam Law Newspaper*. Retrieved from <https://baophapluat.vn/canh-bao-o-nhiem-moi-truong-do-dot-rom-ra-post350503.html>, accessed on 19 July 2023.
- Morya R., Andrianantenaina F.H., Singh S., Pandey A.K., Kim G.-B., Verma J.P., Kumar G., Raj T., Kim S.-H., 2023. Exploring rice straw as substrate for hydrogen production: Critical challenges and opportunities. *Environmental Technology & Innovation*, 31103153.
- Mountrakis G.I.J., Ogole C., 2011. Support vector machines in remote sensing: A review. *ISPRS Journal of Photogrammetry and Remote Sensing*, 66(3), 247–259.
- Narzary A., Brahma J., Das A.K., 2023. Utilization of waste rice straw for charcoal briquette production using three different binder. *Cleaner Energy Systems*, 5100072.
- Ndikumana E., Ho T.M.D., Nguyen H.T.D., Baghdadi N., Courault D., Hossar L., Moussawi I.E., 2018. Estimation of Rice Height and Biomass Using

- Multitemporal SAR Sentinel-1 for Camargue, Southern France. *Remote Sensing*, 10(9), 1394.
- Nemmour H., Chibani Y., 2006. Multiple support vector machines for land cover change detection: An application for mapping urban extensions. *ISPRS Journal of Photogrammetry and Remote Sensing*, 61(2), 125–133.
- Nguyễn C.T., 2018. Inventory of emissions from burning rice husks and straws in the Southwest region. In, *Environmental Sciences Faculty*. Hanoi: Hanoi University of Natural Resources and Environment, p.105.
- Nguyễn V.K., 2021. Modeling the change of land covers due to flooding in the Mekong Delta using remote sensing and GIS data. In, *Cartography and Remote Sensing*. Ha Noi: University of Mining and Geology, p.132.
- Nguyen V.L., Tateishi R., Nguyen T.H., To T.T., Le M.S., 2014. An analysis of forest biomass changes using geospatial tools and ground survey data: a case study in Yok Don national park, Central Highlands of Vietnam. *Vietnam J. Earth Sci.*, 36(4), 439–450. <https://doi.org/10.15625/0866-7187/36/4/6432>.
- Nguyễn V.T., Nguyễn Đ.H., Trần Q.B., 2018. Relationship between backscattering of Sentinel-1 radar image and NDVI index of Sentinel-2 optical image: a case study for dipterocarp forest in Dak Lak province. *Journal of Forestry Science and Technology*, 3167–176.
- Paneque-Gálvez J., Mas J.-F., Moré G., Cristóbal J., Orta-Martínez M., Luz A.C., Guèze M., Macía M.J., Reyes-García V., 2013. Enhanced land use/cover classification of heterogeneous tropical landscapes using support vector machines and textural homogeneity. *International Journal of Applied Earth Observation and Geoinformation*, 23(1), 372–383.
- Phạm T.H., 2015. Multiple Linear Regression, Nonlinear Regression, and Applications. In, *University of Natural Science*. Hanoi: Hanoi National University, p.106.
- Pham T.M.T., 2019. Research on emissions inventory for rice straw open burning in An Giang province. *Journal of Science and Technology in Civil Engineering*, 13(1), 100–108.
- Pham T.T., Chu T., Tran B.Q., 2024. Modelling spatial patterns of forest fire occurrence in the Northwestern region of Vietnam. *Vietnam J. Earth Sci.*, 46(2), 282–302. <https://doi.org/10.15625/2615-9783/20366>.
- Quân M., 2019. Biomass pellets: Contribute to reducing air pollution. *Hanoi News*. Retrieved from <http://hanoimoi.com.vn/tin-tuc/khoa-hoc/950734/vien-nen-sinh-khoi-gop-phan-giam-ohiem-khong-khi>, accessed on 15 July 2023.
- Sodhi H.S., 2019. Application of Remote Sensing for Above-Ground Biomass Estimation. *International Journal of Science and Research*, 10(4), 182–187.
- Ta B.H., Phung M.L., Kieu G.N., Dang B.H., Nguyen M.Q., 2010. Sources of agricultural rice straw and world experience on treatment and utilization. In, *Summary of Science - Technology - Economics 2010*. Hanoi: National Agency for Science and Technology Information, p.50.
- Takano M., Hoshino K., 2018. Bioethanol production from rice straw by simultaneous saccharification and fermentation with statistical optimized cellulase cocktail and fermenting fungus. *Bioresources and Bioprocessing*, 5(1), 16.
- Tran X.T., Doan T.N.P., Le T.N., Nhu V.H., Bui D.T., 2023. A novel HHO-RSCDT ensemble learning approach for forest fire danger mapping using GIS. *Vietnam J. Earth Sci.*, 45(3), 338–356. <https://doi.org/10.15625/2615-9783/18500>.
- Vi A., 2021. Quoc Oai: The strength of locality is the lever to build a new countryside. *Environmental Magazine*. Retrieved from <http://tapchimoitruong.vn/bao-ve-moi-truong-trong-xay-dung-nong-thon-moi-54/quoc-oai-the-manh-cua-dia-phuong-la-don-bay-xay-dung-nong-thon-moi-25576>, accessed on 19 July 2023.
- Wilhelm K., 2008. *Encyclopedia of Public Health*. Dordrecht. Springer, 1, 1601.
- Xiong Y., Zhang Z., Chen F., 2010. Comparison of artificial neural network and support vector machine methods for urban land use/cover classifications from remote sensing images A Case Study of Guangzhou, South China. In, *ICCAISM 2010 - 2010 International Conference on Computer Application and System Modeling*. Taiwan: IEEE, 13–52.